Landscape-scale modeling of carbon cycling under the impact of soil redistribution: The role of tillage erosion

Kristof Van Oost,[1] Gerard Govers,[2] Timothy A. Quine,[1] Goswin Heckrath,[3] Jorgen E. Olesen,[3] Steven De Gryze,[4] and Roel Merckx[4]

Received 3 February 2005; revised 15 July 2005; accepted 25 August 2005; published 15 November 2005.

[1] Despite its global significance, soil-atmosphere carbon (C) exchange under the impact of soil redistribution remains an unquantified component of the global C budget. Here we use radionuclide and soil organic carbon (SOC) data for two agricultural fields in Europe to undertake a spatial analysis of sediment and SOC fate during erosion and deposition in agricultural uplands. C fluxes induced by soil redistribution are quantified by incorporating C dynamics in a spatially distributed model including both water- and tillage-induced soil redistribution (SPEROS-C). The SOC patterns predicted by SPEROS-C are in good agreement with field observations and show that in upland areas, tillage erosion and deposition exerts a large influence on SOC redistribution and soil profile evolution at a timescale of a few decades. The formation of new SOC at eroding sites and the burial of eroded SOC below plough depth provide an important mechanism for C sequestration on sloping arable land in the order of 3–10 g C m^{-2} yr^{-1}. Any attempt to manage agricultural land to maximize sequestration must fully account for erosion, burial and fate of eroded and buried SOC across the landscape and must also account for the correlation between tillage and erosion.

Citation: Van Oost, K., G. Govers, T. A. Quine, G. Heckrath, J. E. Olesen, S. De Gryze, and R. Merckx (2005), Landscape-scale modeling of carbon cycling under the impact of soil redistribution: The role of tillage erosion, *Global Biogeochem. Cycles*, *19*, GB4014, doi:10.1029/2005GB002471.

1. Introduction

[2] There is now growing recognition that anthropogenically induced changes in soil erosion may play an important role in the global C budget. However, diametrically opposed propositions that erosion represents a source of atmospheric C [*Lal et al.*, 2004] and that it represents a net sink [*Stallard*, 1998] have been postulated. The proposition that soil erosion by water may result in a source of atmospheric C is largely based on the assumption that water erosion accelerates mineralization of SOC mainly owing to the breakdown of aggregates. *Lal* [2003] has suggested that this could represent a significant source of atmospheric CO_2 of 0.8–1.2 Pg C yr^{-1}. In contrast, other authors claim that soil erosion-induced mineralization of SOC is minimal, on the basis of the observation that the concentration of SOC in sediment reservoirs matches that in soils from the contributing watersheds, [*Ritchie*, 1989; *Smith et al.*, 2001].

[3] The proposition that soil erosion may result in a net sink of atmospheric C is largely based on evaluation of the fate of SOC in depositional environments. *Schimel et al.* [1985] and *Stallard* [1998] suggested that the burial of eroded SOC in depositional areas may substantially constrain the SOC decomposition process. The extent to which soil redistribution leads to an atmospheric C sink depends not only on the amount of buried C but also on how much of the C removed at eroding sites is replaced by newly produced SOC through dynamic replacement [*Harden et al.*, 1999]. *Stallard* [1998] analyzed a range of scenarios for global sedimentation and estimated that C burial and dynamic replacement may constitute a net C sink of 0–2.0 Pg C yr^{-1}.

[4] The role of soil erosion within the global C budget may therefore be significant but is highly uncertain, as it is sensitive to the balance between (1) increased mineralization of eroded SOC during and after transport and (2) the combination of reduced mineralization in depositional areas and dynamic replacement at eroding sites. Consequently, an overall C budget at the watershed scale requires an integrated spatial analysis of the fate of eroded SOC during transport, the impact of soil erosion on the SOC remaining at eroding sites and the transport and burial of SOC at depositional sites.

[5] Recently, biogeochemical models that are capable of simulating the impact of soil erosion and/or deposition on SOC storage patterns and C dynamics at a single point

[1]Hydrology and Earth Surface Processes Research Group, University of Exeter, Exeter, UK.
[2]Physical and Regional Geography Research Group, Katholieke Universiteit Leuven, Leuven, Belgium.
[3]Danish Institute for Agricultural Sciences, Tjele, Denmark.
[4]Laboratory for Soil and Water Management, Katholieke Universiteit Leuven, Heverlee, Belgium.

0886-6236/05/2005GB002471

Table 1. Field Site Characteristics

	Saeby	Coombe Barton
Field size, ha	3.9	4.1
Number of ^{137}Cs/SOC samples	133/112	245/245
Date of sampling, month/year	04/1998	10/1997
Reference Inventory/±1 std. dev., Bq m^{-2}	2430/±329	2500/±100
Clay ±1 std. dev., [a] %	30 (±12)	14.9 (±2)
Sand ±1 std. dev., [a] %	39 (±12)	40.7 (±6)
Crops	cereals/beets	cereals/grass
Mean annual temp., °C/precip., mm	7.4/666	10.3/845

[a]Data for 0–0.25 m soil layer.

[*Harden et al.*, 1999; *Manies et al.*, 2001; *Liu et al.*, 2003] or the landscape scale [*Rosenbloom et al.*, 2001] have been developed. However, an overall budget of C at the watershed scale has not been made and it is often implicitly assumed that water (i.e., rainfall) induced soil redistribution is the single active process. However, the last decade has seen a paradigm shift in soil erosion research with the identification and growing acceptance of the dominant role of tillage in redistributing soil within sloping arable fields in many different agro-environments [*Govers et al.*, 1999]. Tillage results in a characteristic soil redistribution pattern of net loss from convexities such as crests and shoulders slopes and net accumulation in concavities such as footslopes and hollows. Tillage redistributes soil in amounts that often dwarf the effect of water induced soil redistribution at the field. Recent estimates of tillage erosion and deposition rates based on the radionuclide caesium-137 (^{137}Cs), which integrate soil redistribution over the period ~1954 to the present, frequently exceed 10 Mg ha^{-1} [e.g., *Quine et al.*, 1997]. Recent studies have shown the importance of tillage for within-field soil variability and concluded that tillage has lead to the removal of substantial amounts of SOC on shoulderslopes and the subsequent transport to footslopes and toeslopes, where deep soils with high SOC inventories develop [e.g., *Pennock and Frick*, 2001; *Van Oost et al.*, 2004]. However, the significance of tillage-induced soil redistribution for soil/atmosphere C exchange and the C cycle in general has hitherto not been evaluated.

[6] In this study, we present SPEROS-C, a spatial explicit, multiple soil layer model that enables the simulation of C dynamics in the entire soil profile and allows for the lateral transfers of soil and SOC between different landscape positions. SPEROS-C is used in conjunction with ^{137}Cs and SOC data from two agricultural field sites in Europe to evaluate the hypothesis that contemporary erosion and deposition, and the associated SOC profile evolution, results in significant C fluxes between the soil and atmosphere and to determine the direction of the net C flux.

2. Materials and Methods

2.1. Sites and Field Measurements

[7] The study sites were on the Saeby farm (57°20′N 10°31′E), located in Northern Jutland, Denmark, and on the Coombe Barton farm (50°51′N 3°35′W), located in Devon, UK. Both sites are small, hydrologically isolated, arable fields with an area of ~4 ha and are used for commercial intensive cropping. The sites have a rolling topography with slopes ranging between 1–23% and 0.5–30% for Saeby and Coombe Barton, respectively. Basic field site characteristics and crop rotations are summarized in Table 1. Soils are classified as Cambisols and Luvisols at Saeby and as Cambisols at Coombe Barton. Soil texture is relatively uniform at the Coombe Barton site, while clay content is variable at Saeby ranging between 10 and 56% in the 0–0.25 m layer. Both sites have been in continuous arable cultivation for at least several decades, but agricultural history may date back several centuries. Mechanized tillage was introduced in 1960 at Saeby and in 1945 at Coombe Barton. The annual tillage cycle includes at least one pass of a moldboard plow and two or more passes of a disk, tine or cultivator harrow.

[8] Our study utilizes the data compiled by *Heckrath et al.* [2005] and *Quine and Zhang* [2002] where soil cores were collected on the basis of a regular grid. The cores were divided into two sections corresponding to the plow layer (0–0.25 m) and the sub-plow layer (~0.25–0.5 m). At Saeby, the sub-plow layer was further divided into two samples. SOC contents and bulk density of these samples were given by *Heckrath et al.* [2005] and *Quine and Zhang* [2002]. For Saeby, the sub-plow values used here were calculated as the average of the two sub-plow layer samples. The ^{137}Cs inventories of the soil profiles (i.e., activity in the soil column per unit area, e.g., Bq m^{-2}) and the reference fallout inventory of ^{137}Cs, obtained by sampling 10 undisturbed and uneroded sites adjacent to the sampled fields, were also measured. Detailed digital elevation models (DEM) of the study sites are also available.

2.2. SPEROS Model

[9] Simulation of soil redistribution within this work is based on the SPEROS model. The most important features of the model are (1) independent simulation of water-induced and tillage-induced soil redistribution, (2) mapping of predictions into space and (3) the low number of parameters used to provide a flexible and transparent model structure. For a full description we refer to *Van Oost et al.* [2003a]. Here we only give a brief overview. Water-induced, i.e., inter-rill and rill, soil detachment are described as a power function of slope gradient and contributing area,

$$E_{ir} = k_1 \rho_b S^a \tag{1}$$

$$E_r = k_2 \rho_b S^b A^c, \tag{2}$$

where E_{ir} and E_r are the detachment by inter-rill and rill processes (kg m^{-2}), respectively. Here ρ_b is the dry bulk density of the soil (kg m^{-3}), S is the slope gradient (m m^{-1}), A is the unit contributing area, i.e., contributing area per unit contour width (m^2 m^{-1}), and k_1, k_2, a, b and c are coefficients. The local detachment rate is considered to equal the sum of the inter-rill and rill detachment unless the local transport capacity is exceeded. The local transport capacity is considered to be directly proportional to the rill detachment. If the local sediment inflow exceeds the

transport capacity, deposition occurs, so that the amount of material transported equals the transport capacity. In some cases, not all the sediment that is produced is redeposited in the same field. The model therefore keeps track of the amount of sediment that leaves the study area.

[10] Tillage results in the translocation and dispersion of the plough layer. Experiments have indicated that during a tillage pass, soil particles are typically displaced in the range 0.1–0.5 m while some are displaced as far as 2 m. The model simulates the redistribution of soil constituents by convoluting the probability distribution of the tillage displacement (G) with the spatial distribution of the soil constituents and the tillage soil redistribution rate (kg m^{-2}) at location (k, l) in a grid-based system is calculated as

$$E_{til}(k,l) = \rho_b D\left[\left(\sum_{x=-\infty}^{+\infty}\sum_{y=-\infty}^{+\infty} G(k-x, l-y)\right) - 1\right], \quad (3)$$

where D is the tillage depth (m). The summation term represents the probability of finding initial soil mass at location (k, l) after a tillage pass. The model also accounts for variation of soil translocation with slope gradient, which is a basic characteristic of tillage, leading to loss or accumulation of soil on specific landscape positions. The tillage displacement distributions are therefore estimated from the local slope as described by *Van Oost et al.* [2003b]. Specific boundary conditions are applied: Field boundaries act as lines of zero-flux, as no soil material is translocated over a field boundary during tillage.

2.3. Caesium-137 as a Soil Redistribution Tracer

[11] The radionuclide ^{137}Cs has been widely used as a sediment tracer since the pioneering work of *Rogowski and Tamura* [1965] and *Ritchie and McHenry* [1975]. It is present in the soil mainly as the result of predominantly wet fallout from aboveground nuclear weapon tests between 1950 and 1970. ^{137}Cs is strongly adsorbed by soil particles, especially the fine fraction, and, in mineral soils, subsequent ^{137}Cs redistribution has almost exclusively occurred in association with sediment transport. Consequently, the spatial distribution of ^{137}Cs at a given time represents the net effect of all soil redistribution processes, which had occurred since fallout began. Quantitative estimates of soil erosion and deposition rates can be obtained by deploying ^{137}Cs conversion models [*Walling and Quine*, 1990]. In this study, we use the conversion model developed by *Van Oost et al.* [2003a]. The model combines a ^{137}Cs mass balance model [*Quine*, 1995], describing the accumulation and depletion of ^{137}Cs at one point in the landscape, with SPEROS. The model exploits the fundamentally different dependency on topography of water and tillage erosion to establish their relative contribution in the total soil redistribution.

[12] Parameter values for the conversion model were the same as those proposed by *Van Oost et al.* [2003a]. As no detailed information on tillage directions during the last 4 decades was available, we assumed that tillage mainly occurred up and downslope in alternating directions. We simulated one pass by moldboard plow, turning soil left and right, and one chisel pass each year. Chernobyl fallout for the Saeby and Coombe Barton sites is negligible owing to low rainfall amounts in April 1986. The conversion model was then applied without a priori assumptions about the intensity of water or tillage soil redistribution. An analysis was performed to explore the water and tillage model parameters at which the model is in close agreement with the observed ^{137}Cs inventories, using the procedures described by *Van Oost et al.* [2003a]. The parameter sets that resulted in a good fit were then used to estimate the intensity of soil redistribution and the relative contribution of water and tillage erosion for each point in the landscape. Soil redistribution rates are representative for the period 1954–1997, which is the period between the start of ^{137}Cs fallout and the date of sampling.

2.4. SPEROS-C Model Description

[13] Here we present the model SPEROS-C that allows a spatial analysis of the movement of eroded soil and associated C toward zones of deposition and its effect on C dynamics throughout the soil profile in agricultural landscapes. Soil redistribution within SPEROS-C is based on the SPEROS model while simulation of C dynamics is based on the Introductory Carbon Balance Model (ICBM) [*Andrén and Kätterer*, 1997], which has been successfully applied to describe C dynamics in long-term agricultural field experiments [*Kätterer and Andrén*, 1999]. The main characteristic of the SPEROS-C model is the three-dimensional representation of the soil landscape. SPEROS-C dynamically keeps track of the evolution of the soil profile and SOC storage under erosion and deposition in a spatial framework. The model uses a time step of 1 year and represents space by a uniform grid of cells (or raster map) and explicitly simulates the pathways of eroded sediment and SOC toward zones of deposition. Each grid cell is symmetric (0.5 × 0.5 m). The model characterizes the soil profile up to 1 m depth using four layers (Figure 1). Concentrations of SOC are assumed to be uniform within one layer and the depth of the plow layer is kept constant at 0.25 m.

2.4.1. Soil Carbon

[14] The ICBM model characterizes the organic C using two state variables (a young (Y) and an old pool (O) (g C m^{-2})). There are four fluxes: (1) input, (2) mineralization from the young pool, (3) mineralization from the old pool and (4) transformation of Y into O. The fluxes are governed by four rate-determining parameters; k_{ty}, k_{to}, h and r. The differential equations describing the dynamics are

$$\frac{dY}{dt} = i - k_{ty} r Y \quad (4)$$

$$\frac{dO}{dt} = h k_{ty} r Y - k_{to} r O, \quad (5)$$

where i is the input of C (g C m^{-2} yr^{-1}), h is the humification coefficient, r is a climate coefficient, and k_{ty} and k_{to} are turnover rates of young and old C pools,

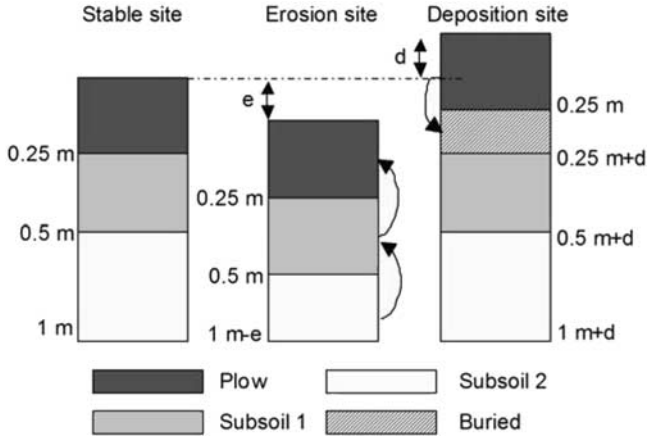

Figure 1. Schematic diagram of model soil profile. The model keeps track of dynamic changes in the soil profile under erosion and deposition. Segments e and d are the erosion and deposition height, respectively.

respectively (year^{-1}). The humification coefficient depends on C source and soil clay content [*Kätterer and Andrén*, 1999].

$$h = \frac{i_c h_c + i_m h_m}{i} e^{0.0112(cl-36.5)} \tag{6}$$

$$i = i_c + i_m, \tag{7}$$

where cl is soil clay content (%), i_c and i_m are inputs of C in (1) crop residues, roots, rhizodeposition and (2) manure (g m^{-2} yr^{-2}), respectively, and h_c and h_m are humification coefficients for crop residues and manure, respectively. The climate effect (r) was assumed to depend on temperature using a correction factor r_T,

$$r_T = 2.07^{\frac{T-5.4}{10}}, \tag{8}$$

where T is annual mean air temperature (°C). The Q_{10} dependency on temperature is based on the mean annual temperature of 5.4°C for the site in Sweden where the k_1 and k_2 values were estimated [*Andrén and Kätterer*, 1997]. The Q_{10} value was taken from *Kätterer et al.* [1998]. The turnover rates for the plough layer were set to k_{ty} = 0.8 year^{-1} and k_{to} = 0.006 year^{-1}, and the humification coefficients were set to h_c = 0.125 and h_m = 0.31 [*Kätterer and Andrén*, 1999]. The turnover times are taken to decrease exponentially with depth (z (m)) [*Rosenbloom et al.*, 2001],

$$k_{tz} = k_{t0} \exp(u_r z), \tag{9}$$

where k_{tz} and k_{t0} are the turnover rates at depth z and 0, respectively. The value of u_r was set to 2.6 so that the turnover time equals 110 years for the 0–0.25 m layer and 900 years for the 0.50–1.0 m layer.

[15] The C input into the soil profile is modeled by an exponential root density profile,

$$\varphi(z) = \begin{cases} 1 & z \le z_r \\ \exp(-c(z - z_r)) & z > z_r \end{cases}, \tag{10}$$

where z is soil depth (m) and z_r is a reference depth, which was set to 0.25 m. The constant c was set to 8, which results in 67% of the root dry matter in the top 1 m depth being in the top 25 cm [*Gerwitz and Page*, 1974]. The proportion of total root dry matter to 1 m depth that can be found in the soil was calculated as

$$p_t = \begin{cases} \dfrac{z_t}{z_r + (1 - \exp(-c(1 - z_r)))/c} & z_t \le z_r \\ \dfrac{z_r + (1 - \exp(-c(z_t - z_r)))/c}{z_r + (1 - \exp(-c(1 - z_r)))/c} & z_t > z_r \end{cases}. \tag{11}$$

[16] Additional C input into the plough layer by residue incorporation and/or manure can be specified.

2.4.2. C Redistribution and Profile Evolution

[17] The SPEROS model is used to calculate the amount of young ($C_{ero,Y}$) or old ($C_{ero,O}$) C eroded from the top layer,

$$C_{ero,Y} = Y_{PD} \frac{M_{ero}}{M_{PD}}, \tag{12}$$

where Y_{PD} is the amount of young SOC in the plough layer (g), M_{ero} is the mass of the eroded soil (g), M_{PD} is the total mass of the plough layer (g). A similar expression is used to calculate the amount of old SOC in the eroded soil. In the case of water-induced soil redistribution, an enrichment factor can be applied to each of the SOC pools to simulate selective erosion/deposition of C. However, in this study we assume that the enrichment factors equal unity. This choice is justified by the fact that (1) the contribution of inter-rill erosion, usually associated with a preferential transport of the finer fractions, to the total sediment production under agricultural erosion may be assumed to be relatively low [*Whiting et al.*, 2001] and (2) most sediment transport on fine-grained soils occurs in the form of relatively stable soil aggregates [*Beuselinck et al.*, 2000; *Rosenbloom et al.*, 2001]. Soil and SOC redistribution by tillage is simulated as a non-selective process. As plough layer depth is maintained, a fraction of SOC from the first subsoil layer is incorporated into the plough layer while some C from the second subsoil layer is assigned to the first subsoil layer, in proportion to the erosion height (Figure 1).

[18] Eroded C is redistributed over the landscape using the SPEROS model. The rate and location of deposition is then used to simulate a change in soil depth. As plough layer depth is maintained, a fraction of the SOC from the plough layer is transferred toward a buried plough layer. The amount of SOC transferred is proportional to the deposition height. The depth of the buried plough layer is dynamic and equals the total deposition height (Figure 1). The subsoil layers are also buried in the soil profile. We

recognize that because SPEROS-C does not simulate the transport of dissolved organic C, there will be modest loses of C that are not accounted for by the model.

[19] There is no reason to expect the soil transport associated with tillage erosion to lead to additional C mineralization and the mineralization caused by tillage independently of transport is accounted for within ICBM in the coefficients k_{ty} and k_o. However, the transport of eroded SOC by water erosion may result in a source of atmospheric C due to the additional mineralization of the displaced SOC [*Lal*, 2003]. A fixed fraction of the C transported in runoff (C_{ero}) is therefore assumed to be mineralized (f_{trans}) so that the C loss due to mineralization of SOC in soil eroded by water (C_{trans}) can be calculated as

$$C_{trans} = C_{ero} * f_{trans}, \quad (13)$$

where f_{trans} is in the range [0.1]. A specific value for f_{trans} can be applied to each of the C pools, i.e., young and old.

[20] It is also possible that a fraction of the eroded soil is exported from the field by water erosion from the study area under consideration, and this must be taken into account when calculating C budgets. This exported C may be deposited on other agricultural fields or may reach the fluvial network. This aspect is not spatially implemented in the model and therefore a k_{exp} term is introduced which allows the user to manipulate the mineralization of the water erosion exported C. When this term equals 1, the exported C is deposited in an environment where it is fully sequestered for example in a wetland. Alternatively, the C exported by overland flow may be assumed to mineralize at rates of depositional areas. The k_{exp} is then calculated as

$$k_{exp} = 1 - \frac{C_E}{C_{Tdepo}}, \quad (14)$$

where C_E is the C efflux from soil to atmosphere due to mineralization of buried C rich material below the plough layer and C_{Tdepo} is the total amount of C deposited in depositional areas (see further).

2.4.3. Comparison With CREEP

[21] The SPEROS-C model design, i.e. a numerical model combining geomorphic processes with models of C dynamics, resembles the CREEP model presented by *Rosenbloom et al.* [2001]. CREEP also adopts a multiple soil layer structure that enables the simulation of C dynamics in the entire profile and allows for the spatial transfers of soil and SOC between different landscape positions. Although SPEROS-C is conceptually similar to the CREEP model, the model domain is substantially different. CREEP simulates gradual diffusive geomorphic processes occurring on undisturbed grasslands such as soil creep, surface wash, biogenic disturbance and eolian transport and the associated textural differentiation. As such, CREEP focuses on the long-term, i.e., century to millennial-scale, hillslope response. In contrast, SPEROS-C simulates contemporary, i.e., anthropogenically accelerated, geomorphic processes occurring on agricultural land: inter-rill, rill and tillage induced soil redistribution. SPEROS-C can be applied at a timescale of a few years to several decades.

Table 2. Observed and Simulated Average C Storage for Saeby and Coombe Barton Field Sites

Field Site	Manure, g C m^{-2}	$C_{0-0.25}$,[a] g C m^{-2}	$C_{0.25-0.5}$,[b] g C m^{-2}	$C_{0.5-1}$,[c] g C m^{-2}
Saeby	40	4758[d]/4795[e]	1618 [d]/1680[e]	1351
Coombe Barton	50	5517[d]/5635[e]	2029[d]/2345[e]	1385

[a]Carbon content for the 0–0.25 m soil layer.
[b]Carbon content for the 0.25–0.5 m soil layer.
[c]Carbon content for the 0.5–1 m soil layer.
[d]Simulated value for the year 2000 using scenario A.
[e]Observed value on non-eroding sites.

2.5. SPEROS-C Model Implementation

[22] The Saeby and Coombe Barton sites used in this study have experienced a long influence of agricultural practices, in the order of several centuries. A detailed reconstruction of the land use, management and erosion history of the sites will therefore be inherently associated with a very high uncertainty. Also, this study focuses on the spatial heterogeneity of the various processes. Additional, non-negligible uncertainties may arise from the unknown original slope profile and heterogeneities in parent material within a field of complex topography when reconstructing the spatial variability of SOC storage and its evolution through time on these sites. Therefore, rather than adopting a full historical approach, we use the following model implementation:

[23] The model is run for the period 1950–2000 using a spatially uniform C content at steady state at the start of the simulation. This implies uniform SOC in the plow layer but not between the different soil layers. We recognize that this is an improbable initial condition, however, it is used because (1) no data are available to determine the actual initial condition; and (2) a uniform initial condition allows the extent of potential change in spatial heterogeneity of SOC to be established and isolates the role of soil redistribution processes. The implications of these assumptions will be considered in the discussion. The steady state SOC contents for the soil profile are based on ICBM parameterization assuming no spatial variation in texture and turnover rates and a constant dry bulk density of 1.35 kg m^{-3} for the 0–0.25m layer and 1.40 kg m^{-3} for the subsoil layers (Table 2). Grain yield increased substantially within this period and we use a linear increase in dry grain yield of 5 g m^{-2} yr^{-1} [*Austin*, 1999; *Utzon-Frank and Andersen*, 2001]. Grain yield was also assumed to be spatially uniform. Several set-up runs without soil redistribution were performed, with adjustment of the annual input of C through manure and initial grain yield to give the best agreement with the observed SOC profile at non-eroding sites (based on ^{137}Cs data). The simulated and observed SOC contents for the various layers, assuming no erosion or deposition, are given in Table 2.

[24] We isolate the effects of soil redistribution on C dynamics from the effects of increasing grain yields by simulating C dynamics under four different soil redistribution intensities scenarios: (A) no erosion/deposition, (B) soil

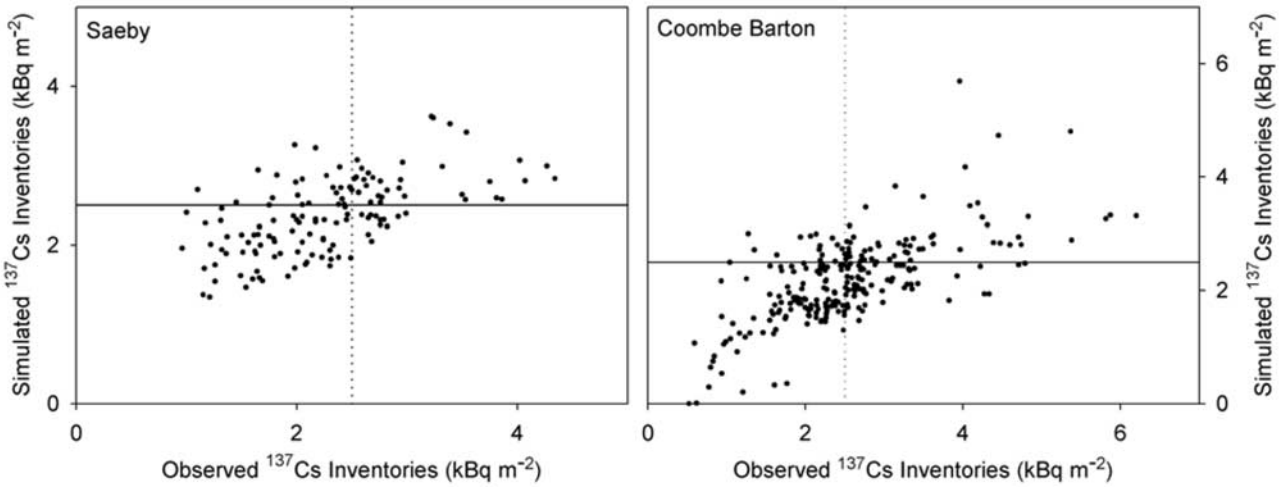

Figure 2. Model evaluation: scatterplot of simulated against observed ^{137}Cs inventories for Saeby (r^2 = 0.40) and Coombe Barton (r^2 = 0.45).

redistribution by water alone, (C) soil redistribution by tillage alone and (D) soil redistribution by both water and tillage. The component of the C fluxes that are the result of soil redistribution are then isolated by subtracting the simulated changes in SOC for Scenario A from those simulated for each of the soil redistribution scenarios (B to D). The intensities of water- and tillage-induced soil redistribution, used in scenarios B to D, are those derived from the ^{137}Cs measurements. Owing to the relative short simulation periods and the range of slope curvatures it is not necessary to include erosion/deposition feedbacks on topography, instead fixed DEM's, based on present-day field surveys, are used. Finally, we assume that 5% of the transported SOC by rainfall-induced soil redistribution is mineralized; that is, f_{trans} equals 0.05 for each of the C pools.

3. Results

3.1. Soil Redistribution Rates

[25] Both sites are characterized by a similar pattern of ^{137}Cs activity: low values (indicating erosion) are found on the shoulder and backslope positions while high values (indicating deposition) occur at the footslopes and hollows (see auxiliary material[1]). The observed patterns of soil redistribution are therefore typical of tillage erosion [*Govers et al.*, 1994]. High rates of tillage erosion are also found at the down-slope side of the field boundaries. This is because substantial amounts of soil are moved downhill on the steep slopes in this area while no soil is transported across the up-slope field boundary. This leads to the formation of a soil step at this location [*Dabney et al.*, 1999], which is also observed in the field.

[26] The SPEROS simulations reproduce the observed spatial patterns well (Figures 2 and 3). Using the SPEROS model, we estimate that at Saeby and Coombe Barton, more than 80% of the total soil redistribution must be attributed to tillage erosion. Field averaged gross soil redistribution rates, i.e., combined tillage and water induced, are estimated at 10.0 and 10.4 Mg ha^{-1} yr^{-1} for Saeby and Coombe Barton, respectively. These values correspond with average soil losses of ~0.07 m from the eroding sites during the period 1950–2000, equivalent to ~28% of 0.25 m plow layer depth. However, only a small fraction (~15%) of the total eroded sediment is exported from both sites by overland flow while all the sediment eroded by tillage is deposited again in the same fields. This leads to substantial soil burial in concave landscape positions. We estimate that average soil accumulation equals c. 0.08 m during the period 1950–2000, equivalent to 32% of the plow layer depth. Note that these are spatially averaged values; local soil loss and accumulation rates may exceed 0.25 m (see Figure 3). This result agrees with earlier studies that have indicated the dominance of tillage in soil redistribution on rolling topography [*Quine et al.*, 1997; *Govers et al.*, 1996].

3.2. SOC Redistribution

[27] Figure 4 shows SPEROS-C simulations of SOC-soil redistribution for both sites, whereby observations of SOC for different soil layers are also indicated. The model simulations replicate in a very reasonable fashion the observed reduction of plow layer SOC content with increasing erosion rates at both sites although it underestimates the SOC contents of depositional areas at Coombe Barton. The model simulates a substantial variation in SOC at eroding sites. This reflects the differences in source areas, which may vary in SOC contents owing to variable erosion rates. In contrast, the model simulates constant SOC concentrations in the plough layer. The eroded C, which has the same SOC content as depositional sites at the beginning of the simulation, is slowly transported toward the depositional areas where decomposition rates and C inputs to the plough layer are similar. This

[1] Auxiliary material is available at ftp://ftp.agu.org/apend/gb/2005GB002471.

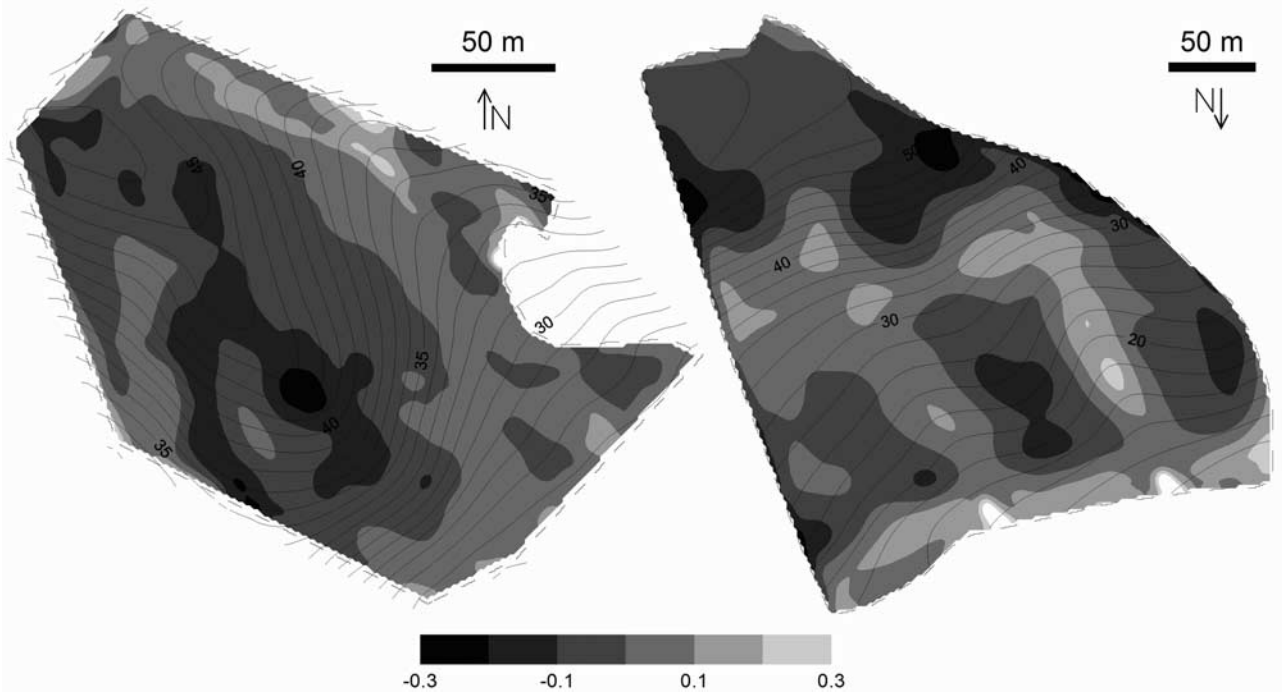

Figure 3. Simulated rates of combined tillage- and water-induced soil redistribution (m/50 yr) based on ^{137}Cs measurements at (left) Saeby and (right) Coombe Barton (negative values indicate erosion; positive values indicate deposition). See color version of this figure in the HTML.

leads to uniform C concentrations in the plough layer at depositional areas.

[28] Despite the variation of subsoil SOC observations, a clear trend toward lower SOC values at eroding landscape positions and higher values at depositional areas is apparent within both sites. The model is able to reproduce this pattern well (Figure 4). However, at both sites, the SOC depletion at eroding sites and SOC gain at depositional sites is under-

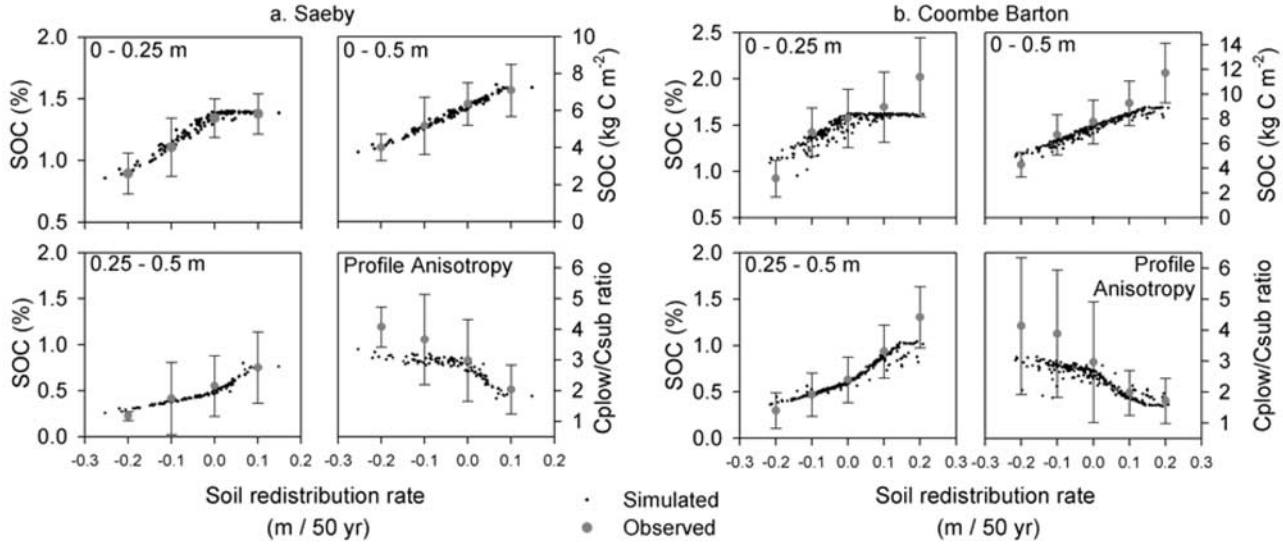

Figure 4. Model evaluation: scatterplot of observed and simulated SOC storage (scenario D) for different soil layers and profile anisotropy against soil redistribution rates (derived from ^{137}Cs data) for (a) Saeby and (b) Coombe Barton. The simulated values are only shown when observed values are available. For clarity, the observed values are grouped into soil redistribution classes of equal width (0.1 m) and the mean and 1 standard deviation are shown. See color version of this figure in the HTML.

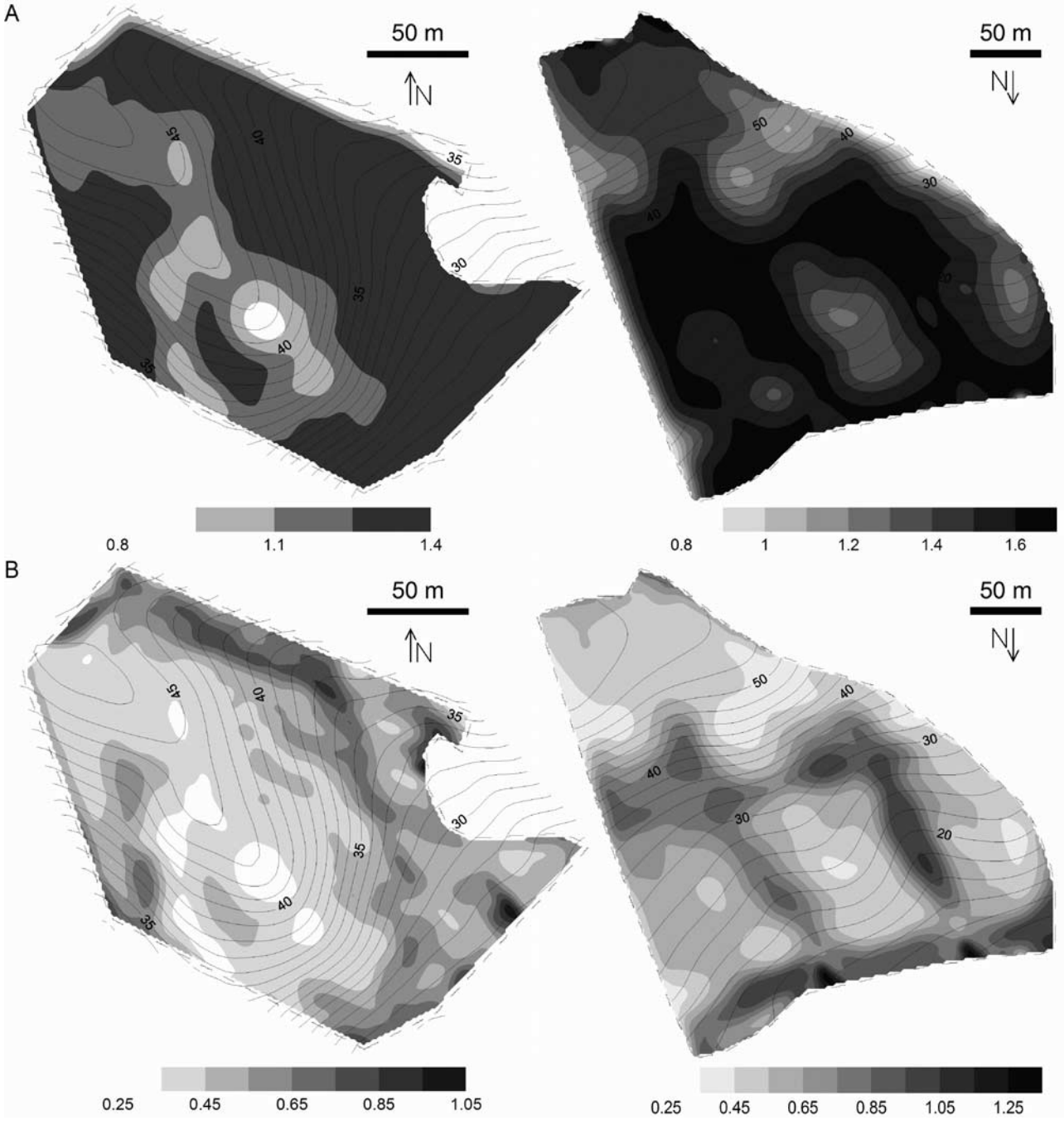

Figure 5. Simulated spatial distributions of SOC storage at (left) Saeby and (right) Coombe Barton (scenario D): (a) 0–0.25 m layer (%) (b) 0.25–0.5 m layer (%). See color version of this figure in the HTML.

estimated for the 0.25–0.5 m layer. The underestimation of subsoil depletion at eroded sites may reflect overestimation in the model of the depth of root penetration at these sites. The underestimation of accumulation at depositional sites may result from the fact that we only simulated a time period of 50 years, starting from a spatial uniform SOC content. The observed values reflect the long soil redistribution history of the sites, which may date back several centuries.

[29] The relation between soil and SOC redistribution can also be evaluated by analyzing differences in SOC profile anisotropy [*Quine and Zhang*, 2002]. Profile anisotropy is expressed as the ratio of SOC concentration in the plow layer to the SOC concentration in the 0.25–0.5 m layer. Again, a clear trend appears (Figure 4). In areas where minimal soil redistribution takes place, the ratio equals ~3. In depositional areas, most of the ratios lie

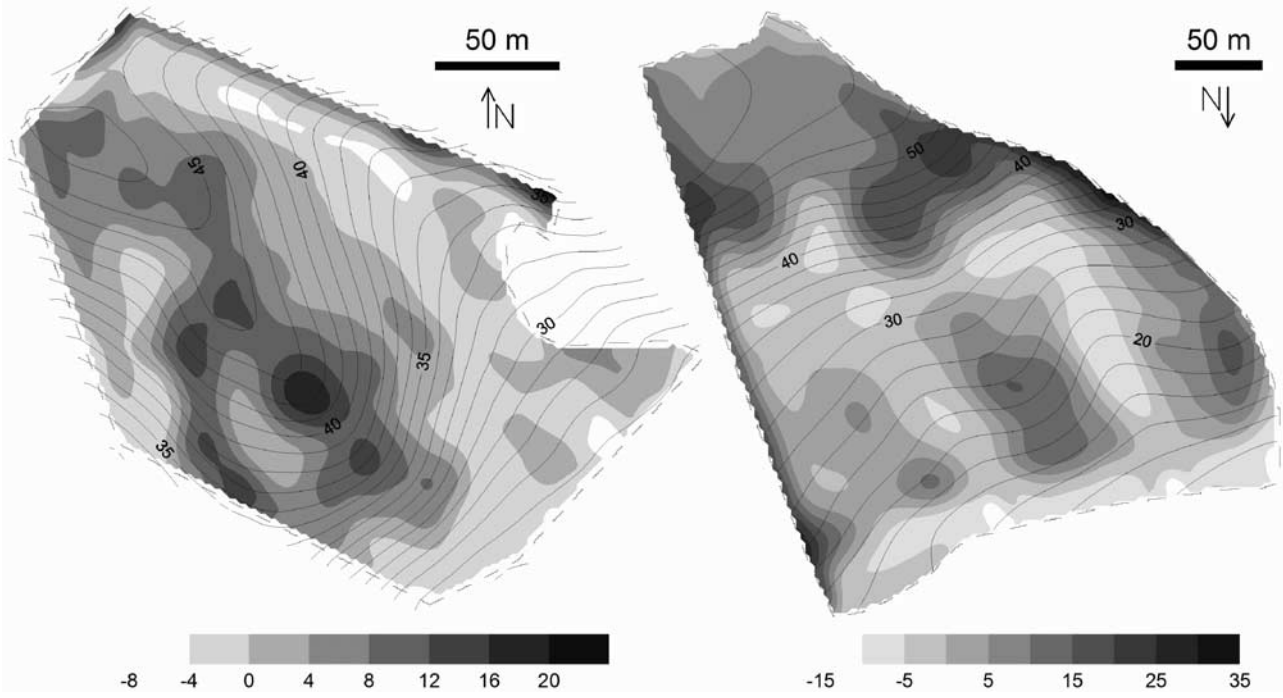

Figure 6. Simulated soil redistribution induced net C flux between soil and atmosphere at (left) Saeby and (right) Coombe Barton (g C m^{-2} yr^{-1}; scenario D). Negative values indicate a net flux to the atmosphere, and positive values indicate a net flux to soils. See color version of this figure in the HTML.

between 1.5 and 3, with a decline toward values as low as 1 as deposition rates increase. This reflects the increasing quantities of former plow soil that is relatively rich in SOC that is buried below the plow layer by gradual surface elevation due to soil deposition. In contrast, at eroding landscape positions, the ratios are much higher and increase from 3 to 4 as erosion rates increase. This reflects the admixture of subsoil low in SOC in the plow layer as the latter is continuously removed owing to erosion. The SOC profile anisotropy patterns predicted by SPEROS-C closely correspond to the observations. However, SPEROS-C underestimates the anisotropy ratios at eroding sites.

[30] The observed patterns of SOC and good correspondence with SPEROS-C simulations strongly supports the hypothesis that SOC and soil redistribution are closely linked. The model simulations indicate that soil redistribution can strongly affect the spatial distribution of SOC storage within a time span of only 50 years (Figure 5). Because of the dominance of tillage-induced soil redistribution, SOC erosion and deposition acts most effectively on regions with high curvature, i.e., removal on divergent shoulders, while valleys and footslopes tend to fill. On eroding sites, plough layer depth is maintained by incorporating SOC-poor subsoil. Over time, the plow layer on these eroded shoulders becomes depleted in SOC (Figure 5a). This implies that plow layer SOC is being eroded more rapidly than it is being replaced by (1) subsoil SOC and (2) fixation of atmospheric C through crop production (see section 1). The proportion of the field that has a severely SOC-depleted plow layer (SOC loss >20%) increases from 0 to ~22% and 18% between 1950 and 2000 for Saeby and Coombe Barton, respectively. Similar depletion rates are obtained for the 0.25–0.5 m soil layer (Figure 5b). In the valleys and on the footslopes a deep soil enriched in SOC develops. The proportion of the field that develops subsoil substantially enriched in SOC (SOC gain >20%) increases from 0 to 31% and 38% between 1950 and 2000 for Saeby and Coombe Barton, respectively. The rate of SOC transfers from the plough layer to the subsoil in depositional areas is substantial and averages 26 g C m^{-2} yr^{-1} for Saeby and 35 g C m^{-2} yr^{-1} for Coombe Barton (see auxiliary material).

3.3. C Sources and Sinks

[31] The mechanisms described above provide the potential for significant fluxes of C between the soil and atmosphere. Figure 6 shows SPEROS-C simulations of net C fluxes between soil and atmosphere for scenario D. Negative values indicate a net flux to the atmosphere, positive values a net flux to soils. It is important to note that the fluxes shown here are only induced by soil redistribution processes and not by management strategies. Erosion invokes an atmospheric sink term: erosion enhances C uptake at the eroding sites through dynamic replacement, i.e., by continuously taking away a fraction of SOC that is replenished with new C input. Conversely, the deposition sites are a net C source to the atmosphere. Here C-rich sediment buried below the plow layer continues to be subject to mineralization, albeit at lower rates, and this

Table 3. Simulated Field-Averaged Fluxes of C Between Soil and Atmosphere for Various Scenarios (g C m^{-2})[a]

Scenario[b]	Site	C_{exp}	C_{trans}	C_E	C_B	C_{Net}[c]
B	Saeby	2.50	−0.17	−0.04	0.85	0.63/0.61
	C Barton	1.39	−0.14	−0.08	0.84	0.62/0.59
C	Saeby	0.0	0.0	−0.33	2.93	2.85/2.85
	C Barton	0.0	0.0	−0.73	4.18	3.44/3.44
D	Saeby	2.12	−0.14	−0.34	3.50	3.30/3.08
	C Barton	1.81	−0.14	−0.74	4.74	3.87/3.84

[a]Negative values indicate a net flux to the atmosphere, positive values a net flux to soils. C_{exp} is the C exported from the field by water erosion; C_{trans} is the flux due to accelerated carbon mineralization by water erosion and; C_E is the flux due to mineralization of buried C; C_B is flux due to dynamic replacement; and C_{net} is the net landscape-scale soil flux between soil and atmosphere.

[b]See text for explanation.

[c]Maximum values indicate net flux when the exported SOC by water erosion is fully sequestered; minimum value indicates net flux when the exported carbon by water erosion is assumed to decompose at rates of depositional areas (equation (14)).

loss of C by mineralization in addition to the mineralization of C in the plough layer is not compensated for by local C return with crop residues, nevertheless, C import with soil leads to SOC accumulation. These observations are in qualitative agreement with previous studies [*Harden et al.*, 1999, 2002; *Manies et al.*, 2001; *Liu et al.*, 2003]. The local sink and source strengths vary between −8 and 22 g C m^{-2} at Saeby and −15 and 33 g C m^{-2} at Coombe Barton. The difference in the sink/source magnitudes between the sites is related to the overall higher SOC content at Coombe Barton.

[32] The spatially distributed SPEROS-C model allows identification and quantification of the various C sources and sinks and their integration at the landscape scale. Landscape-scale values have been determined for each scenario for each of the following sources and sinks: (1) C_E, the C efflux from soil to atmosphere due to mineralization of buried C rich material below the plough layer, (2) C_B, the C flux from atmosphere to soil due to dynamic replacement, (3) C_{exp}, the C exported from the field by water erosion, (4) C_{trans}, the C flux from soil to atmosphere due to accelerated C mineralization during and after transport by water erosion and (5) C_{net}, the net landscape-scale soil flux between soil and atmosphere (negative values indicate a source of atmospheric C, positive values a sink) induced by soil redistribution. The landscape-averaged fluxes of C are obtained by simulating C fluxes due to soil redistribution at various positions in the landscape and are presented in Table 3. For each soil redistribution scenario (B to D), the field average flux values represent the spatial integration of all grid cell values of the difference in the simulated flux between that obtained with the soil redistribution scenario and that obtained with scenario A (the no soil redistribution scenario).

[33] For each of the scenarios (water only, tillage only and water and tillage soil redistribution), the model simulates absolute values of the C_B term that are greater than the absolute values of the C_E term. This indicates that for all scenarios, the acceleration of dynamic replacement as a result of erosion exceeds the increased mineralization of buried C in the sub-plow layer. This is due to the fact that turnover rates in the top layer, where eroded SOC is being replaced, are typically higher than turnover rates in the subsoil, where SOC is more effectively protected from decomposition. Thus, once buried out of the plow layer, subsoil SOC is relatively well preserved.

[34] The model predicts that under water-induced soil redistribution alone (scenario B), a net small sink may be created, even though 5% of the erosion mobilized SOC is mineralized (Table 3). However, a fraction of the eroded SOC is exported from the fields and this may further reduce/increase the sink strength, depending on the fate of the eroded SOC. No soil is exported from the field by tillage-induced soil redistribution and no increased mineralization of SOC occurs during or after transport (scenario C). The final balance is therefore controlled by C dynamics at erosional and depositional sites within the field. As the admixture of C-poor subsoil at sites eroded by tillage leads to rapid C fixation while the SOC that is buried at depositional sites is slowly mineralized, soil redistribution by tillage always leads to a net C uptake at the landscape scale (3−4 g C m^{-2}). The C-fluxes induced by tillage are also substantially higher than those induced by water erosion. This is due to the fact that tillage soil redistribution rates are much higher than water soil redistribution rates on these arable fields (see section 3.1).

4. Discussion

[35] Although the SPEROS-C simulations are in good agreement with the observed SOC patterns, the discrepancies between simulated and observed profile anisotropy (Figure 4) suggest some interesting issues. The significant difference between the simulated and measured profile anisotropy ratios on eroding sites might be caused by a number of factors. Pre-agricultural soil redistribution may have created a template for plant productivity and SOC patterns [e.g., *Schimel et al.*, 1985; *Rosenbloom et al.*, 2001]. Our model implementation, assuming spatial uniform SOC patterns, implies that we do not address the issue of pre-existing (i.e., pre-1950s) history. We tested the effect of the pre-1950s soil redistribution impacts at Coombe Barton by increasing the simulation period until a steady state is reached, that is, when C_{net} remains constant (scenario E). Note that the patterns generated by tillage-induced soil redistribution, which is the dominant soil redistribution process on our sites, closely resemble those generated by natural diffusive, geomorphic processes [*Rosenbloom et al.*, 2001]. This equilibrium was obtained after ∼200 simulation years and resulted in a better prediction of the plow-subsoil SOC ratios. At Coombe Barton, the average ratio for eroding sites increased from 2.6 (scenario D) to 3.0 (scenario E). This is still much lower than the observed ratio of 3.7 (Figure 4). However, increasing the simulation period substantially increased the strength of the soil redistribution-induced C sink, C_{net}. Using scenario E, SPEROS-C simulates field-averaged C uptake in the order of 10.1 g C m^{-2} yr^{-1} (compare with 3.8 g C m^{-2} yr^{-1} using scenario D). Ongoing soil redistribution rates result in a larger difference between subsoil and plow layer SOC contents, which

in turn results in increased rates of dynamic replacement (C_B) while the C efflux (C_E) at depositional sites remains relatively constant. This suggests that our estimates of dynamic replacement, and hence C_{net}, are probably conservative.

[36] C input through primary production in SPEROS-C is spatially homogeneous and is not affected by landscape position or erosion. Studies have shown that patterns of yield show a close similarity to soil redistribution patterns [*Kosmas et al.*, 2001; *Quine and Zhang*, 2002; *Heckrath et al.*, 2005] and higher C input from plant can be expected in sites of soil deposition. In addition, soil erosion may result in a loss of net primary production [*McCarty and Ritchie*, 2002]. This could also explain the substantial underestimation of SOC storage at depositional sites at Coombe Barton (Figure 4). Other SPEROS-C model parameters and input data (e.g., texture, bulk density, SOC turnover rates) were also assumed to be spatially homogeneous. Temperature, soil moisture, texture and aeration are the principal determinants of SOC mineralization rates. These environmental factors all vary both considerably in the horizontal (i.e., with geographical location) and in the vertical (i.e., with depth in a soil profile) dimension.

[37] Soil temperature and moisture are closely related with topography [e.g., *Moore et al.*, 1991] and may interact with the dynamics introduced by soil redistribution. Implementation of these factors requires the reliable estimation of temperature and wetness but also their effect on C dynamics. Many C models have functions to describe the effect of water content and temperature on microbial processes. In combination, these models could be used to derive spatial maps of an extended climatic variable r in the C module. Incorporation of spatially variable parameters and feedback mechanisms between soil redistribution, texture, primary production and water dynamics must be the next step in model development, to completely account for the impact of soil redistribution on soil-atmosphere C exchange at the landscape scale.

[38] Traditionally, soil scientists have focused on the upper soil profiles when examining the controls of organic matter dynamics [e.g., *Andrén and Kätterer*, 1997], although significant amounts of C are stored below this layer. While the controls over soil carbon dynamics are well established for the upper layers, controls over decomposition rates in the lower soil profile remain poorly understood. Use of exponential downscaling of turnover rates with soil depth in this study implicitly defines how temperature, moisture, aeration, etc., influence turnover throughout the soil profile. However, further experimental verification and mechanistic modeling [e.g., *Liu et al.*, 2003] of this concept could substantially increase our understanding of C dynamics under the impact of soil redistribution.

[39] Finally, we tested the effect of transport-related mineralization due to water-induced soil redistribution (f_{trans}). Increasing values for f_{trans} resulted in decreasing SOC contents in depositional areas as a fixed portion of the transported SOC is directly mineralized. Values higher than 0.05 resulted in a substantial underestimation of the SOC contents in depositional areas. This suggests that the value range of 0.2–0.35, proposed by *Jacinthe and Lal* [2001] and *Lal* [2003], is probably an overestimation for our sites.

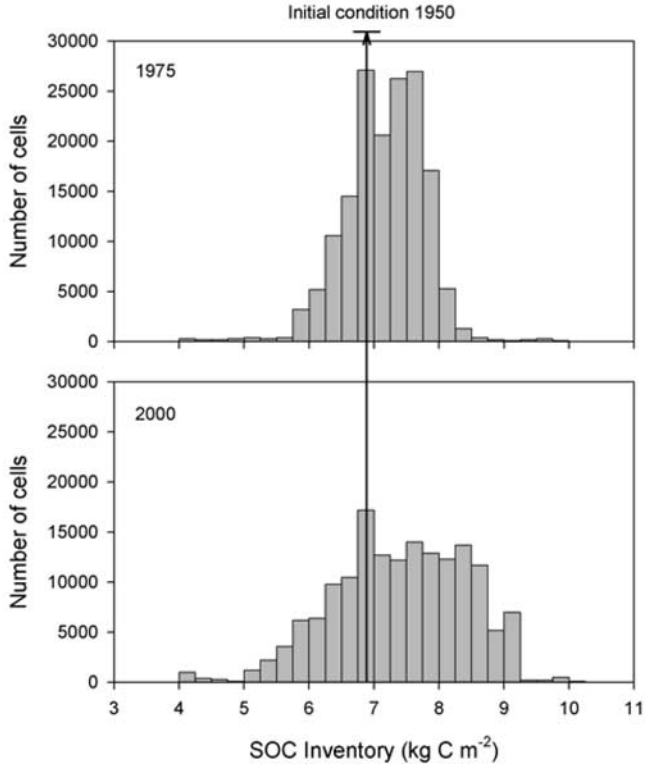

Figure 7. Areal distribution of SOC storage for the 0–0.5 m layer at Coombe Barton as affected by soil redistribution between 1950 and 2000 (scenario D).

5. Implications and Conclusions

[40] In this study, we presented a model that allows simulation of the effect of both water- and tillage-induced soil redistribution processes on C storage and fluxes on arable land. The SOC patterns predicted by SPEROS-C are in good agreement with field observations, suggesting that the model captures the dynamics of the various processes involved rather well. Our model simulations clearly show that soil redistribution can strongly affect the spatial distribution of SOC storage. The histograms in Figure 7 show the spatial redistribution of SOC after 25 and 50 simulation years. Clearly, continuing soil redistribution results in more extreme spatial variability in SOC storage. In particular, greater SOC depletion on the shoulders is anticipated. However, in contrast to earlier estimates [e.g., *Lal*, 2003], this does not represent a loss of SOC to atmospheric CO_2. Instead, our spatial analysis of sediment and SOC fate during erosion and deposition show that agricultural uplands exhibit a net gain of SOC in the order of 3–10 g C m^{-2} yr^{-1}. The formation of new SOC on eroding sites and the burial of eroded SOC below plough depth provide an important mechanism for C sequestration.

[41] The data and model results strongly suggest that tillage is the dominant soil redistribution process on these sites and plays an important role in C cycling on arable land. However, until now, the correlation between tillage and erosion and deposition were not explicitly considered in studies assessing the effect of soil redistribution on C dynamics. Although tillage erosion is a relatively new area of research (first articles appeared in the 1990s), tillage erosion has been documented in many areas throughout the world. Tillage erosion experiments provide consistent results and allow prediction of tillage soil redistribution rates with a relatively high precision. The relative importance of tillage in the total soil redistribution is illustrated the Canadian Agri-Environmental Indicator Project [*McRae et al.*, 2000], which is at present the only attempt to assess the significance of tillage erosion at the regional scale. It was concluded that approximately 50% of the cropland in Canada was subject to unsustainable levels of tillage erosion (>6 Mg ha^{-1} yr^{-1}) while only approximately 15% of the cropland was subject to unsustainable levels of water erosion. Equivalent data are not available for other regions. These findings, together with our model simulations and the globally widespread occurrence of tillage certainly warrant further investigation of the role of tillage-induced soil redistribution in the terrestrial C balance.

[42] Recognition and understanding of the magnitude and dynamics of the soil redistribution induced C sink is important for land management adjustment to maximize C sequestration. For example, the C sequestration potential of conversion from conventional to no-tillage systems must fully account for erosion, burial and fate of eroded and buried SOC across the landscape and must also account for the correlation between tillage and erosion. Therefore this study highlights the need both to reassess the role of arable land in the C cycle and to re-evaluate the methodologies proposed for source reduction and sink optimization.

[43] **Acknowledgments.** We gratefully acknowledge the support of the European Commission under the Marie Curie IntraEuropean Fellowship Programme. The contents of this work reflect only the author's views and not the views of the European Commission.

References

Andrén, O., and T. Kätterer (1997), ICBM: The introductory carbon balance model for exploration of soil carbon balances, *Ecol. Appl.*, *7*, 1226–1236.

Austin, B. E. (1999), Yield of wheat in the United Kingdom: Recent advances and prospects, *Crop Sci.*, *39*(6), 1604–1610.

Beuselinck, L., A. Steegen, G. Govers, J. Nachtergaele, I. Takken, and J. Poesen (2000), Characteristics of sediment deposits formed by intense rainfall events in small catchments in the Belgian Loam Belt, *Geomorphology*, *32*, 69–82.

Dabney, S. M., Z. Liu, M. Lane, J. Douglas, J. Zhu, and D. C. Flanagan (1999), Landscape benching from tillage erosion between grass hedges, *Soil Tillage Res.*, *51*, 219–231.

Gerwitz, A., and E. R. Page (1974), An empirical mathematical model to describe plant root systems, *J. Appl. Ecol.*, *11*, 773–781.

Govers, G., K. Vandaele, P. Desmet, J. Poesen, and K. Bunte (1994), The role of tillage in soil redistribution on hillslopes, *Eur. J. Soil Sci.*, *45*, 469–478.

Govers, G., T. A. Quine, P. J. J. Desmet, and D. E. Walling (1996), The relative contribution of soil tillage and overland flow erosion to soil redistribution on agricultural land, *Earth Surf. Processes Landforms*, *21*, 929–946.

Govers, G., D. A. Lobb, and T. A. Quine (1999), Tillage erosion and translocation: Emergence of a new paradigm in soil erosion research, *Soil Tillage Res.*, *51*, 167–174.

Harden, J. W., J. M. Sharpe, W. J. Parton, D. S. Ojima, T. L. Fries, T. G. Huntington, and S. M. Dabney (1999), Dynamic replacement and loss of soil carbon on eroding cropland, *Global Biogeochem. Cycles*, *13*, 885–901.

Harden, J. W., T. L. Fries, and M. J. Pavich (2002), Cycling of beryllium and carbon through hillslope soils in Iowa, *Biogeochemistry*, *60*, 317–335.

Heckrath, G., J. Djurhuus, T. A. Quine, K. Van Oost, G. Govers, and Y. Zhang (2005), Tillage erosion and its effect on soil properties and crop yield in Denmark, *J. Environ. Qual.*, *34*, 312–324.

Jacinthe, P. A., and R. Lal (2001), A mass balance approach to assess carbon dioxide evolution during erosional events, *Land Degrad. Dev.*, *12*, 329–339.

Kätterer, T., and O. Andrén (1999), Long-term agricultural field experiments in northern Europe: Analysis of the influence of management on soil carbon stocks using the ICBM model, *Agric. Ecosyst. Environ.*, *72*, 165–179.

Kätterer, T., M. Reichstein, O. Andrén, and A. Lomander (1998), Temperature dependence of organic matter decomposition: A critical review using literature data analyzed with different models, *Biol. Fertil. Soils*, *27*, 258–262.

Kosmas, C., S. Gerontidis, M. Marathianou, B. Detsis, T. Zafiriou, W. Nan Muysen, G. Govers, T. Quine, and K. Vanoost (2001), The effects of tillage displaced soil on soil properties and wheat biomass, *Soil Tillage Res.*, *58*, 31–44.

Lal, R. (2003), Soil erosion and the global carbon budget, *Environ. Int.*, *29*, 437–450.

Lal, R., M. Griffin, J. Apt, L. Lave, and M. G. Morgan (2004), Managing soil carbon, *Science*, *304*(5669), 393, doi:10.1126/science.1093079.

Liu, S. G., N. Bliss, E. Sundquist, and T. G. Huntington (2003), Modeling carbon dynamics in vegetation and soil under the impact of soil erosion and deposition, *Global Biogeochem. Cycles*, *17*(2), 1074, doi:10.1029/2002GB002010.

Manies, K. L., J. W. Harden, L. Kramer, and W. J. Parton (2001), Carbon dynamics within agricultural and native sites in the loess region of western Iowa, *Global Change Biol.*, *7*, 545–555.

McCarty, G. W., and J. C. Ritchie (2002), Impact of soil movement on carbon sequestration in agricultural ecosystems, *Environ. Pollut.*, *116*, 423–430.

McRae, T., C. A. S. Smith, and L. J. Gregorich (2000), Environmental sustainability of Canadian agriculture: Report of the Agri-Environmental Indicator Project, report, 224 pp., Agric. and Agri-Food Can., Ottawa.

Moore, I. D., R. B. Grayson, and A. R. Ladson (1991), Digital terrain modelling: A review of hydrological, geomorphological, and biological applications, *Hydrol. Processes*, *5*, 3–30.

Pennock, D. J., and A. H. Frick (2001), The role of field studies in landscape-scale applications of process models: An example of soil redistribution and soil organic carbon modeling using CENTURY, *Soil Tillage Res.*, *58*, 183–191.

Quine, T. A. (1995), Estimation of erosion rates from caesium-137 data: The calibration question, in *Sediment, Water Quality in River Catchments*, edited by I. D. L. Webster et al., pp. 307–329, John Wiley, Hoboken, N. J.

Quine, T. A., and Y. Zhang (2002), An investigation of spatial variation in soil erosion, soil properties, and crop production within an agricultural field in Devon, United Kingdom, *J. Soil Water Conserv.*, *57*, 55–65.

Quine, T. A., G. Govers, D. E. Walling, X. B. Zhang, P. J. J. Desmet, Y. S. Zhang, and K. Vandaele (1997), Erosion processes and landform evolution on agricultural land—New perspectives from caesium-137 measurements and topographic-based erosion modelling, *Earth. Surf. Processes Landforms*, *22*, 799–816.

Ritchie, J. C. (1989), Carbon content of sediments of small reservoirs, *Water Resour. Bull.*, *25*, 301–308.

Ritchie, J. C., and J. R. McHenry (1975), Fallout Cs-137: A tool in conservation research, *J. Soil Water Conserv.*, *30*, 283–286.

Rogowski, A. S., and T. Tamura (1965), Movement of ^{137}Cs by runoff, erosion and infiltration on the alluvial Captina silt loam, *Health Phys.*, *11*, 1333–1340.

Rosenbloom, N. A., S. C. Doney, and D. S. Schimel (2001), Geomorphic evolution of soil texture and organic matter in eroding landscapes, *Global Biogeochem. Cycles*, *15*, 365–381.

Schimel, D. S., D. C. Coleman, and K. A. Horton (1985), Soil organic matter dynamics in paired rangeland and cropland toposequences in North-Dakota, *Geoderma*, *36*, 201–214.

Smith, S. V., W. H. Renwick, R. W. Buddenmeier, and C. J. Crossland (2001), Budgets of soil erosion and deposition for sediments and sedimentary organic carbon across the conterminous United States, *Global Biogeochem. Cycles*, *15*, 697–707.

Stallard, R. F. (1998), Terrestrial sedimentation and the carbon cycle: Coupling weathering and erosion to carbon burial, *Global Biogeochem. Cycles*, *12*, 231–257.

Utzon-Frank, T., and B. Andersen (2001), Nature and Environment 2001—Selected indicators, report, 63 pp., Miljøministeriet (Dan. Min. of the Environ.), Copenhagen.

Van Oost, K., G. Govers, and W. Van Muysen (2003a), A process-based conversion model for caesium-137 derived erosion rates on agricultural land: An integrated spatial approach, *Earth. Surf. Processes Landforms*, *28*, 187–207.

Van Oost, K., G. Govers, W. Van Muysen, G. Heckrath, and T. A. Quine (2003b), Simulation of the redistribution of soil by tillage on complex topographies, *Eur. J. Soil Sci.*, *54*, 63–76.

Van Oost, K., G. Govers, T. A. Quine, and G. Heckrath (2004), Comment on "Managing soil carbon" (I), *Science*, *305*, 1567b.

Walling, D. E., and T. A. Quine (1990), Calibration of caesium-137 measurements to provide quantitative erosion rate data, *Land Degrad. Rehab.*, *2*, 161–175.

Whiting, P. J., E. C. Bonniwell, and G. Matisoff (2001), Depth and areal extent of sheet and rill erosion based on radionuclides in soils and suspended sediment, *Geology*, *29*, 1131–1134.

S. De Gryze and R. Merckx, Laboratory for Soil and Water Management, Katholieke Universiteit Leuven, Kasteelpark Arenberg 20, 3001 Heverlee, Belgium.

G. Govers, Physical and Regional Geography Research Group, Katholieke Universiteit Leuven, Redingenstraat 16b, 3000 Leuven, Belgium.

G. Heckrath and J. E. Olesen, Danish Institute for Agricultural Sciences, 8830 Tjele, Denmark.

T. A. Quine and K. Van Oost, Hydrology and Earth Surface Processes Research Group, University of Exeter, Amory Building, Rennes Drive, EX4 4RJ, UK. (k.vanoost@exeter.ac.uk)